2021 IEEE Custom Integrated Circuits Conference (CICC) | 978-1-7281-7581-2/20/$31.00 ©2021 IEEE | DOI: 10.1109/CICC51472.2021.9431464

A 28GHz Hybrid-Beamforming Transmitter Array Supporting Concurrent Dual Data Steams and Spatial Notch Steering for 5G MIMO

Yaolong Hu*, Xiaohan Zhang*, Taiyun Chi

Rice University, Houston, TX

*Equally-Credited Authors (ECAs)

Spatial multiplexing, or multi-user MIMO, can improve the communication throughput by simultaneously supporting multiple spatially non-collocated data streams. Most multi-user MIMO TRXs at GHz are based on digital beamforming. However, as the data rate of each user approaches multi-Gb/s at mmWave, performing dynamic beamforming weights calculation in digital and high-speed digital-to-analog conversion faces a significant energy efficiency bottleneck for large-scale mmWave antenna arrays. Alternatively, hybrid beamforming can support a handful of concurrent data streams by combining analog beamforming with digital precoding. Although hybrid beamforming loses degrees-of-freedom compared to all-digital processing, it reduces digital computation complexity and the number of digital-to-analog conversion chains, resulting in greatly enhanced energy efficiency.

One remaining challenge for hybrid-beamforming base station TX is to perform spatial notch steering in addition to beamforming, which is critical to suppress interferences to the RX devices in the network. For example, a uniform four-element TX array with random mismatches among the four elements (±1dB amplitude and ±10° phase mismatches) has a sidelobe level of only -10dB (Fig. 1a). If the sidelobe of data stream #1 happens to align with the main lobe of data stream #2, it serves as a strong co-channel interference to the far-field RX #2 (Fig. 1a), thus limiting the spatial multiplexing performance. Note that increasing the number of antennas in a uniform array, e.g., from four to 128, only leads to a mild rejection for the first sidelobe, from -11.3 to -13.3dB. Dolph-Chebyshev windowing is a common technique to suppress the sidelobes, as shown in Fig. 1c. The problem is that Dolph-Chebyshev arrays require non-uniform element amplitudes with some channels working in the backoff region (Fig. 1d), leading to significant main-beam power degradation (as large as 3.1dB for -35dB sidelobe level).

In this paper, we present a spatial notch filtering technique to complement existing hybrid-beamforming TX. As shown in Fig. 2, there are K parallel RF processing channels within one antenna element, each consisting of two phase-shifting paths. The signal beamforming is performed by the main-path phase shifters, as in conventional hybrid beamformers. Meanwhile, the auxiliary-path phase shifters form an interference-canceling beam with scaled amplitude and 180° phase shift. A spatial notch can then be synthesized towards an arbitrary nulling direction by spatially combining the main beam and interference-canceling beam. Compared to Dolph-Chebyshev arrays, the amplitudes of all the antenna elements are set as full strength in the proposed notch steering scheme. In addition, when nulling the sidelobes, the main lobe is aligned with the sidelobe of the interference-canceling beam (Fig. 2), offering minimal power and beamwidth degradation to the main lobe. We verify the proposed technique using a four-element array simulation (Fig. 1b). Two spatial notches are created for data stream #1 and #2, respectively, enabling dual-data-stream transmission without interference. The array factor degradation of the main lobe is only 0.68dB, ensuring the full strength of the TX radiated signal. As the auxiliary-path phase shifters require signal attenuation instead of gain, additional auxiliary paths can be added with little dc power overhead if more spatial notches are needed.

As a proof-of-concept demonstration, we implement a 28GHz four-element dual-data-stream hybrid-beamforming TX array in a 45nm CMOS SOI process. The schematic of main-path and auxiliary-path phase shifters is shown in Fig. 3. After one-to-four power splitting, each data stream is processed by a differential I/Q generation network, followed by main-path and auxiliary-path I/Q VGAs. The outputs of the two data streams are combined using a transformer-based parallel power combiner and further amplified by a three-stage PA. For the VGA design, the binary-weighted cells are implemented as differential cascode amplifiers and controlled by tail switches (Fig. 3). When S is logic high (or low), the left (or right) branch turns on and generates an output current with "+" (or "-") polarity. This topology guarantees constant input and output parasitic capacitances, since the input and output terminals are always loaded by an "on" and an "off" differential pair regardless of the VGA settings. A half-bit unit cell is used to generate +1/0 weight with the differential outputs of its right branch tied to V_{DD}. Overall, the normalized gain of the 5-bit VGA can be set as any integer from -15 to +16. The auxiliary-path VGAs are implemented using the same topology as the main path with a 60% smaller transistor size.

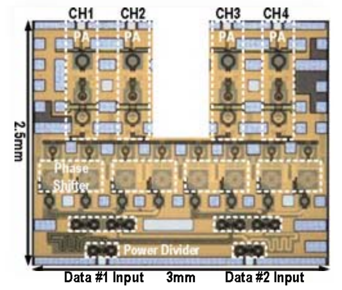

Die micrograph.

The four TX channels are sequentially probed in the measurements. In the small-signal testing (Fig. 4a), S_{21} of the two data streams are well-matched with a 3dB bandwidth of 26.2 - 31.1GHz. S_{11} remains below -10dB from 22.5 to 31.0GHz for both data streams. The swept-power measurement results across frequency are summarized in Fig. 4b–4d. The two data streams present very similar large-signal performance, with 19.7dBm OP_{1dB}, 20.4dBm P_{SAT}, 27.9% PAE at OP_{1dB}, and 30.6% peak PAE at 29GHz (Fig. 4b), demonstrating state-of-the-art TX output power, efficiency, and linearity performance. From 24 to 31GHz, each TX channel achieves >18.6/20.1dBm OP_{1dB}/P_{SAT} and >22.2%/26.5% PAE at OP_{1dB}/P_{SAT}.

Next, we evaluate the phase-shifting performance of the main path and auxiliary path by programming the I/Q VGAs (Fig. 5). When measuring the main-path (or auxiliary-path) constellation, the gain of the I/Q VGAs in the other path is set to be zero. In addition, the output power in the constellation measurements is backed off by 9dB from OP_{1dB}, which resembles the averaged output power of amplifying two independent single-carrier 16-/64-QAM signals each with ~6dB PAPR. From the measured constellations of all the four channels, we can select the main-path phase shifter settings for beamforming and auxiliary-path phase shifter settings for notch steering. After we pick up the desired settings, we reprogram the chip, probe the outputs of the four channels sequentially, and synthesize the array factors in MATLAB. The synthesized array factors of the data stream #1 when the main beam is steered towards 0°, 30°, and 60° are shown in Fig. 5c, Fig. 6a, and Fig. 6b, respectively. We also plot the array factors when a spatial notch is created for one sidelobe, achieving >40.1dB notch depth and <0.7dB main-beam power degradation in all three cases. Finally, we fix the main beam at 0° and steer the spatial notch from -90° to +90° with 1° resolution. Outside the main-beam -10dB beamwidth (-22° to +22°), the achieved notch depth remains >35dB and the main-beam power degradation remains <0.7dB.

In summary, this paper reports a RF-domain spatial notch steering technique for mmWave multi-user MIMO that can realize deep spatial notches while ensuring the full strength of the main beam. A four-element TX array prototype is implemented at the 28GHz 5G band, supporting concurrent dual data streams in the same polarization, with state-of-the-art TX output power, efficiency, and linearity performance (Fig. 6c).

References:

[1] B. Sadhu *et al.*, "A 28-GHz 32-Element TRX Phased-Array IC With Concurrent Dual-Polarized Operation and Orthogonal Phase and Gain Control for 5G Communications," JSSC, Dec. 2017.

[2] S. Mondal *et al.*, "Power-Efficient Design Techniques for mm-Wave Hybrid/Digital FDD/Full-Duplex MIMO Transceivers," JSSC, Aug. 2020.

[3] S. Mondal *et al.*, "A 28/37GHz Scalable, Reconfigurable Multi-Layer Hybrid/Digital MIMO Transceiver for TDD/FDD and Full-Duplex Communication," ISSCC, Feb. 2020.

[4] A. Nafe *et al.*, "2 × 64-Element Dual-Polarized Dual-Beam Single-Aperture 28-GHz Phased Array With 2 × 30 Gb/s Links for 5G Polarization MIMO," TMTT, Sept. 2020.

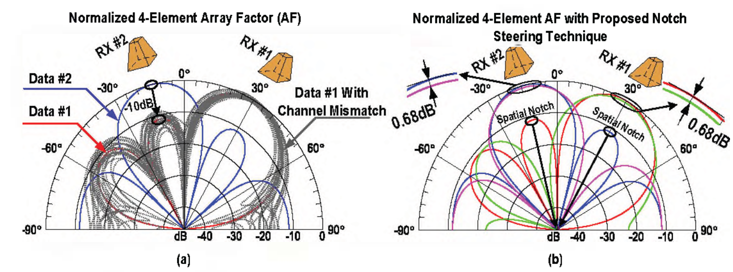

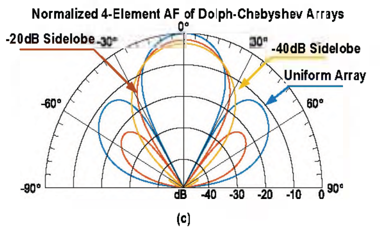

Summary of Dolph-Chebyshev Arrays

Sidelobe Level (dB)	Element Amplitudes	Main-beam Power Degradation (dB)
-10	[1.00, 0.88, 0.88, 1.00]	0.54
-20	[0.58, 1.00, 1.00, 0.58]	2.07
-30	[0.43, 1.00, 1.00, 0.43]	2.92
-35	[0.39, 1.00, 1.00, 0.39]	3.12
-40	[0.37, 1.00, 1.00, 0.37]	3.26

(d)

Fig. 1. Four-element array factors of a uniform array, Dolph-Chebyshev arrays, and the proposed spatial notch steering scheme.

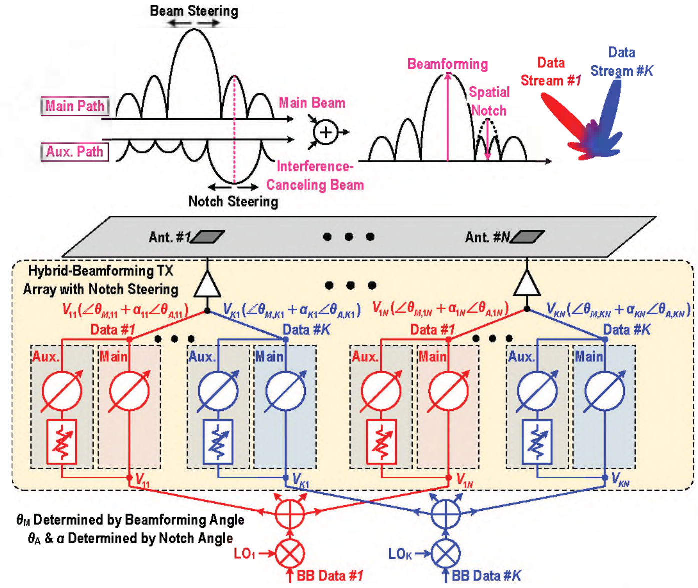

Fig. 2. Proposed TX notch steering technique.

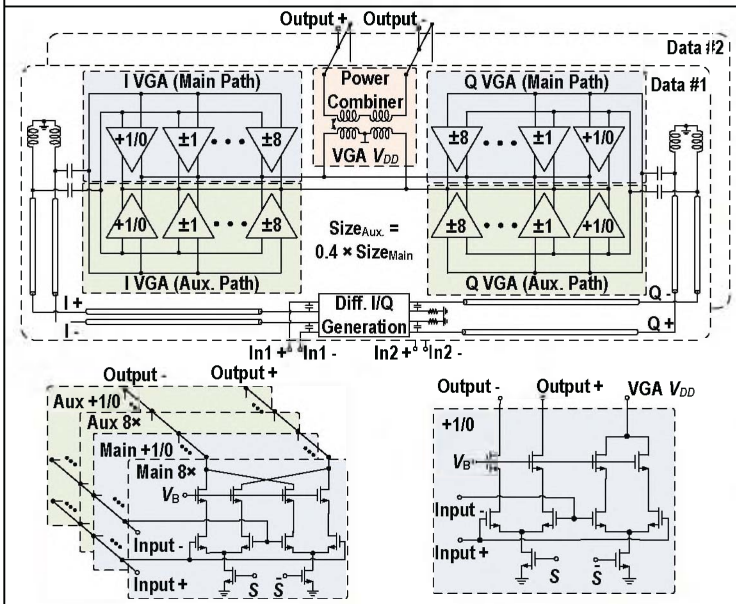

Fig. 3. Schematic of the main- and auxiliary-path phase shifters.

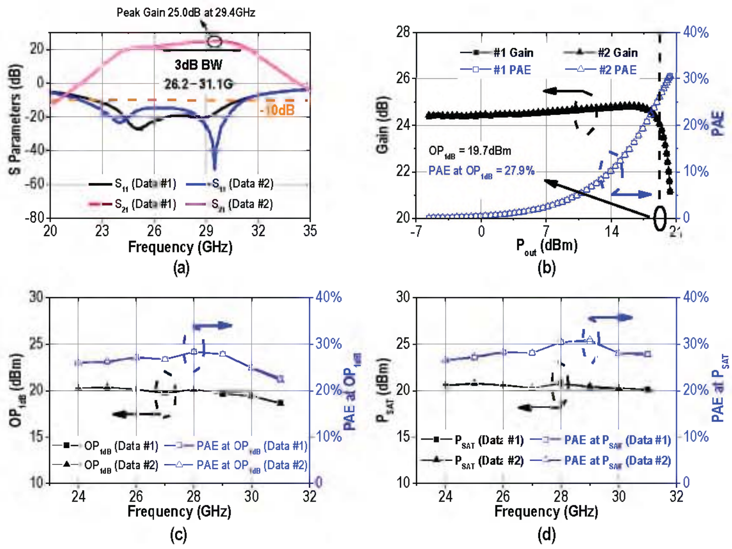

Fig. 4. (a) S_{11}/S_{21} measurements. (b) Swept-power measurements at 29GHz. (c) and (d) OP_{1dB}, P_{SAT}, and PAE over frequency.

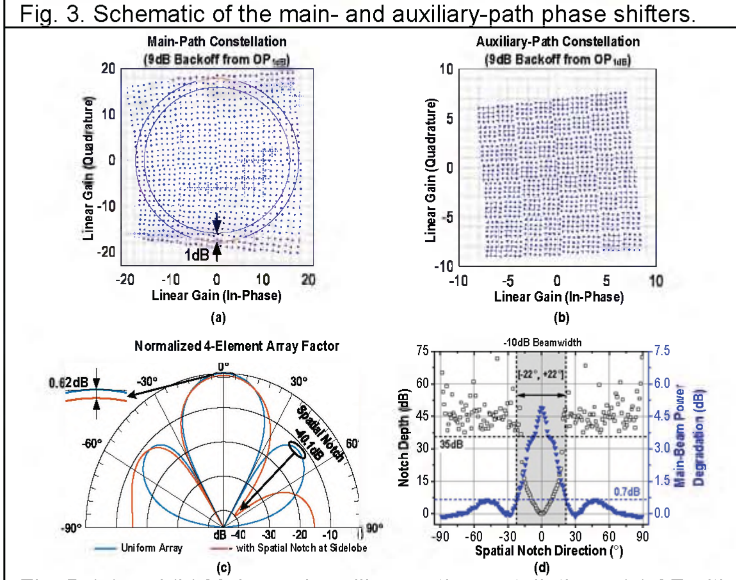

Fig. 5. (a) and (b) Main- and auxiliary-path constellations. (c) AF with and without a spatial notch for 0° beamforming. (d) Notch depth and Main-beam power degradation when steering the notch.

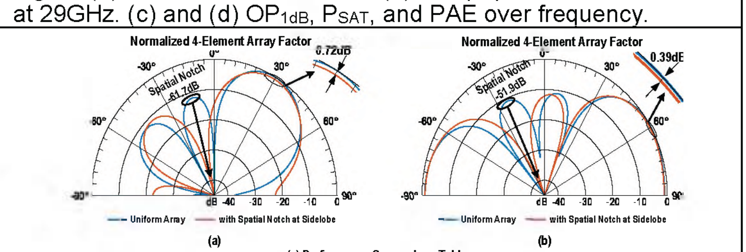

(c) Performance Comparison Table

	[1] JSSC 2017	[2] JSSC 2020	[3] ISSCC 2020	[4] TMTT 2019	This Work
Beamforming Architecture	Analog	Hybrid	Hybrid	Analog	**Hybrid**
# of Data Streams	2 (Dual-Polarization)	2	2	2 (Dual-Polarization)	**2**
Notch Steering	No	Yes (for RX)	Yes (for RX)	No	**Yes (for TX)**
# of Elements per Chip	32 TRX (16H + 16V)	4 TRX	8 TRX	8 TRX (4H + 4V)	**4 TX**
TX Output Power per Channel	16dBm (P_{SAT}) 13.5dBm (OP_{1dB})	15.8dBm (P_{SAT}) 14.1dBm (OP_{1dB})	15.5dBm (P_{SAT}) 14dBm (OP_{1dB})	11-12dBm (OP_{1dB})	**20.4dBm (P_{SAT}) 19.7dBm (OP_{1dB})**
TX Efficiency per Channel	20.5%[a]	20%[b]	21%[b]	7.2%[c]	**27.8% (OP_{1dB}) 30.6% (P_{SAT})**
Frequency (GHz)	28	28/37/39	28/37	28 - 32	**28 (3dB BW: 26.2 - 31.1)**
Technology	130nm SiGe	65nm CMOS	65nm CMOS	180nm SiGe BiCMOS	**45nm CMOS SOI**

[a] Peak Efficiency (PA + Switch + Off-Mode LNA) [b] PA PAE at P_{SAT} [c] PAE Calculated at OP_{1dB} Based on Table I (PA + VGA + Phase Shifter + Switch)

Fig. 6. (a) and (b) AF with and without a spatial notch for 30° and 60° beamforming. (c) Comparison with 28GHz TX arrays.

Preflight Results

Document Overview

Title: A 28GHz Hybrid-Beamforming Transmitter Array Supporting Concurrent Dual Data Streams and Spatial Notch Steerin
Author:
Creator: PScript5.dll Version 5.2.2
Producer: Acrobat Distiller 9.0.0 (Windows); modified using iText® 7.1.9 ©2000-2019 iText Group NV (IEEE; licensed version)

Preflight Information

Profile: Convert to PDF/A-1b
Version: Qoppa jPDFPreflight v2020R2.01
Date: Jul 19, 2021 1:51:36 PM

Legend: (X) - Can NOT be fixed by PDF/A-1b conversion.
(!X) - Could be fixed by PDF/A-1b conversion. User chose to be warned in PDF/A settings.

Page 2 Results

- (X) Font Helvetica does not define all referenced glyphs.
- (X) Font Helvetica does not define all referenced glyphs.
- (X) Font Helvetica does not define all referenced glyphs.
- (X) Font Helvetica does not define all referenced glyphs.
- (X) Font Helvetica does not define all referenced glyphs.
- (X) Font Helvetica does not define all referenced glyphs.
- (X) Font Helvetica does not define all referenced glyphs.